AIAA Guidance, Navigation, and Control Conf., Toronto, Ontario, Canada, 2010

Pursuit and Evasion: Evolutionary Dynamics and Collective Motion

Darren Pais* and Naomi E. Leonard†

Princeton University, Princeton, NJ, 08544, U.S.A.

Pursuit and evasion strategies are used in both biological and engineered settings; common examples include predator-prey interactions among animals, dogfighting aircraft, car chases, and missile pursuit with target evasion. In this paper, we consider an evolutionary game between three strategies of pursuit (classical, constant bearing, motion camouflage) and three strategies of evasion (classical, random, optical-flow based). Pursuer and evader agents are modeled as self-propelled steered particles with constant speed and strategy-dependent heading control. We use Monte-Carlo simulations and theoretical analysis to show convergence of the evolutionary dynamics to a pure strategy Nash equilibrium of classical pursuit vs. classical evasion. Here, evolutionary dynamics serve as a powerful tool in determining equilibria in complicated game-theoretic interactions. We extend our work to consider a novel pursuit and evasion based collective motion scheme, motivated by collective pursuit and evasion in locusts. We present simulations of collective dynamics and point to several avenues for future work.

I. Introduction

Pursuit and evasion behaviors, widely observed in nature, play a critical role in predator foraging, prey survival, mating and territorial battles in several species. Pursuit-evasion contests were studied extensively by Isaacs[1] from a game-theoretic perspective in the context of differential games. In engineering, pursuit and evasion games have received much attention, particularly in the context of missile guidance and avoidance[2,3] and aircraft pursuit and evasion.[4,5] The book by Nahin[6] provides a review of the topic along with relevant historical background.

The pervasiveness of pursuit and evasion in nature suggests the examination of winning strategies from an evolutionary perspective. Here one can think of a strategy as a control law that a particular pursuer (evader) employs to capture (escape). Correlates of evolutionary 'fitness' (fitness is proportional to reproductive or survival rate), such as time-to-capture, provide natural metrics that connect the dynamics of individual pursuer-evader pairs to evolutionary dynamics of populations comprising individuals playing different strategies. Stable equilibria or winning strategies of such evolutionary dynamics (sometimes called evolutionarily stable strategies or ESS[7]) point to strategies or behaviors one would expect to observe in nature. Further, such strategies are often solutions (Nash equilibria) to constrained optimization problems, or to games with complicated structure such as stochastic payoff matrices.

Recently, Wei et al.[8] used the evolutionary approach to study pursuit games, with dynamics derived in the paper by Justh and Krishnaprasad.[9] The authors[8,9] use Monte-Carlo simulations and analytical calculations to study three pursuit strategies competing against a field of deterministic or random nonreactive evasive strategies. The three chosen pursuit strategies (classical, constant bearing and motion camouflage) are biologically inspired. The authors show convergence of an evolutionary dynamics game between the three strategies to pure motion camouflage and motivate this result by empirical observations of hoverflies, dragonflies and bats[10] applying this technique.

In the present paper we build on the work in Ref. 8 by studying the *coevolution* of the three strategies of pursuit from Ref. 8 playing against three distinct evasive strategies, two of which are *reactive* strategies. We use Monte-Carlo simulations and theoretical analysis to show convergence to an equilibrium of classical

*Ph.D. Candidate, Mechanical and Aerospace Engineering, J-32 Engineering Quadrangle, and AIAA Student Member.

†Edwin S. Wilsey Professor, Mechanical and Aerospace Engineering, D-234 Engineering Quadrangle.

pursuit versus classical evasion. We point out that extending the 'games against nature' approach[8] to competitions between two sets of strategies does not result in a motion camouflage as the winning pursuit strategy, as in Ref. 8. Indeed, the environment of evasive strategies that a pursuer population encounters is critical in determining the winning pursuit strategy. As a result, analysis of strategy spaces different again from those studied in the present paper will yield other interesting evolutionary outcomes.

We further explore the winning strategies (classical pursuit and classical evasion) in a collective motion model with agents pursuing and evading designated neighbors on a cyclical interaction topology. This work is motivated by collective motion in cannibalistic locusts[11] and has strong parallels to prior work in cyclic pursuit.[12–14] Simulation results suggest a rich set of solutions for this collective motion model.

The outline of this paper is as follows. Section II describes the planar dynamics for pursuit and evasive agents and the different pursuit and evasion strategies under consideration. In Section III we study the evolutionary dynamics of the two populations. Section IV focuses on the collective motion model with the winning strategies. We conclude and provide directions for future work in Section V .

NOTATION: For notational convenience, the Euclidean plane $\mathbb{R}^2$ is identified with the complex plane $\mathbb{C}$. Thus $(x, y) \in \mathbb{R}^2 \equiv x+iy \in \mathbb{C}$. For two complex numbers $c_1, c_2 \in \mathbb{C}$, the complex inner product is defined as $\langle c_1, c_2 \rangle := \mathrm{Re}(c_1 c_2^*)$, the real part of $c_1 c_2^*$, where c_2^* is the complex conjugate of c_2. $|c_1|$ is the complex modulus of c_1. $\mathbf{1}_N$ represents an $N \times 1$ vector of ones. The (i, j) element of a matrix A is denoted a_{ij}. M^T denotes the transpose of matrix M and $M^{\#}$ denotes the element-wise inverse of M, i.e. $m_{ij}^{\#} = 1/m_{ij}$. For a column vector $\boldsymbol{x}$, x_j denotes the j'th element of $\boldsymbol{x}$.

II. Dynamics of Pursuit and Evasion

We study a two-agent planar pursuit and evasion problem where each agent is modeled as a self-propelled steered particle with constant speed and with angular velocity determined by the interaction between the particles. We consider three pursuit behaviors: *classical*, *constant bearing* and *motion camouflage*, and three evasive behaviors: *classical*, *random motion*, and *optical-flow based*.[15] The choice of the three pursuit behaviors is motivated by work in Refs. 8 and 9, where it is proved that if the speed of the pursuer is greater than that of the evader, the pursuer captures the evader in finite time. Here 'capture' means that the Euclidean distance between the pursuer and evader reaches a designated minimum. Consider a pursuer and an evader moving on the complex plane with positions $r_P = x_P + iy_P \in \mathbb{C}$ and $r_E = x_E + iy_E \in \mathbb{C}$ and headings $\theta_P \in \mathbb{S}^1$ and $\theta_E \in \mathbb{S}^1$, respectively. The dynamics of the two-agent system are given by

$$\begin{aligned} \dot{r}_P &= e^{i\theta_P}, \qquad \dot{\theta}_P = u_P \\ \dot{r}_E &= \nu e^{i\theta_E}, \qquad \dot{\theta}_E = u_E. \end{aligned} \tag{1}$$

Here, the speed of the pursuer is normalized to be 1 and the evader has a constant positive speed $\nu < 1$. We define the *baseline vector*[8] r as the relative position of pursuer with respect to evader, i.e.,

$$r = r_P - r_E.$$

Figure 1 shows the positions and velocity vectors for each particle and the baseline vector. Note that $\dot{r} = e^{i\theta_P} - \nu e^{i\theta_E}$. We define the three *pursuit control laws* following Ref. 8 (with some change of notation):

- Classical pursuit:

$$u_P = -\eta \left\langle \frac{r}{|r|}, i e^{i\theta_P} \right\rangle - \frac{1}{|r|} \left\langle \frac{r}{|r|}, i\dot{r} \right\rangle, \tag{P1}$$

  where η is a constant gain.

- Constant bearing pursuit:

$$u_P = -\eta \left\langle \frac{r}{|r|}, i e^{i\phi} e^{i\theta_P} \right\rangle - \frac{1}{|r|} \left\langle \frac{r}{|r|}, i\dot{r} \right\rangle, \tag{P2}$$

  where $\phi \in (-\pi/2, \pi/2)$ is a chosen constant bearing angle.

- Motion camouflage pursuit:

$$u_P = -\mu \left\langle \frac{r}{|r|}, i\dot{r} \right\rangle, \tag{P3}$$

  where μ is a constant gain.

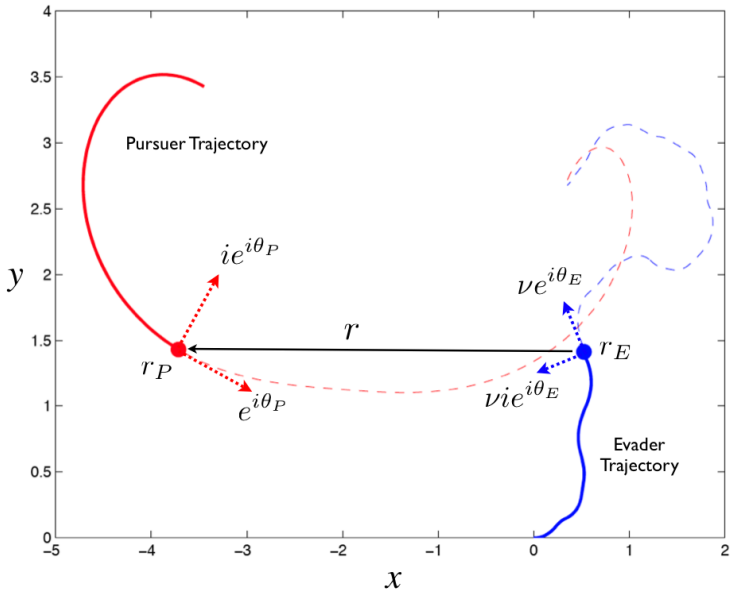

Figure 1. Cartoon trajectories of a pursuer and an evader. Pursuer position r_P and evader position r_E at time t are shown as circles. The corresponding velocities $e^{i\theta_P}$ and $\nu e^{i\theta_E}$ (and the vectors $ie^{i\theta_P}$ and $\nu ie^{i\theta_E}$ normal to these) are shown as dotted arrows. Also shown is the baseline vector r.

We define the three *evasion control laws* as follows:

- Classical evasion:

$$u_E = -\eta \left\langle \frac{r}{|r|}, ie^{i\theta_E} \right\rangle, \tag{E1}$$

  where η is a constant gain.

- Random motion evasion:

$$\begin{aligned} &\text{Piecewise linear paths with turns every } \alpha \text{ time units, and} \\ &u_E \text{ selected uniformly randomly from } [-\kappa, \kappa] \text{ at every turn.} \end{aligned} \tag{E2}$$

- Optical-flow based evasion:

$$u_E = -\eta \tan^{-1}\left(\dot{\theta}\right), \tag{E3}$$

  where θ is the complex argument of r and $\dot{\theta} = -\frac{1}{|r|^2}\langle r, i\dot{r}\rangle$.

Intuitively, classical pursuit (evasion) involves the pursuer (evader) aligning its velocity vector with the baseline. In constant bearing pursuit, the pursuer maintains a constant bearing angle ϕ between its velocity vector and the baseline, whereas in motion camouflage, the pursuer contracts the magnitude of the baseline, while leaving the argument of the baseline unchanged. In Refs. 8, 9, the authors use elegant geometric ideas to show that the pursuit control laws (P1)-(P3) provably correspond to the desired pursuit strategies described above. This is done by defining pursuit manifolds for each strategy ('states of the interacting system that satisfy particular relative position and velocity criteria') and proving convergence to these manifolds for sufficiently high gains η and μ. In optical-flow based evasion, the evader reacts to the changes in the argument of the baseline vector; these changes are intended to mimic optical flow generated by the pursuer on the retina of the evader.[15] Figure 2 shows a simulation of the three pursuit and three evasion strategies pitted against one another. Note that the baseline vectors remain roughly parallel in each case of motion camouflage pursuit (bottom row of panels in Figure 2). The evader trajectory in optical-flow based evasion is a straight line when competing against a motion camouflage pursuit strategy.

For all control laws u_P and u_E defined above, Proposition 1 ensures that capture is always possible in finite time.

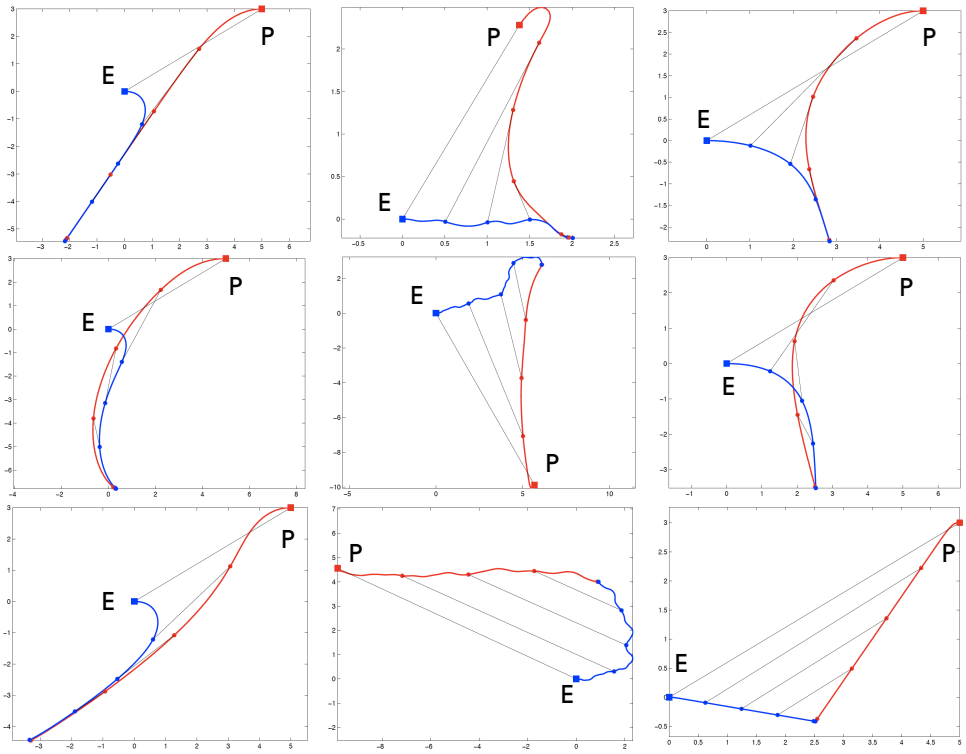

Figure 2. Simulated trajectories of each of the nine pairs of competing pursuit and evasive strategies. The rows correspond to pursuit control laws (P1), (P2) and (P3) respectively and the columns correspond to evasive control laws (E1), (E2) and (E3) respectively. For example, the plot in the middle corresponds to constant bearing pursuit vs. random motion evasion. The starting positions are indicated with 'P' and 'E'. In all plots the evader starts at the origin with $\theta_E(0) = 0$. The pursuers in columns 1 and 3 start at $r_P(0) = 5 + 3i$ with a heading $\theta_P(0) = \pi$. In the second column the pursuers start at random orientations and with random headings. The straight lines in each plot are snapshots of the baseline vector at specific points in time.

Proposition 1. *Consider dynamics* (1) *and control laws (P1)-(P3) and (E1)-(E3). For every capture radius* $\epsilon > 0$ *and every initial condition* $r_P(0)$, $r_E(0)$ *such that* $|r(0)| = |r_P(0) - r_E(0)| > \epsilon$, *there exists a finite capture time* T *such that* $|r(T)| = \epsilon$.

Proof. Refer to Refs. 8, 9 for proof. Note that the evasive controls (E1)-(E3) satisfy the continuity and boundedness assumptions so that the proof extends to these cases. □

The central question we ask in this paper is which strategies win out in a coevolutionary contest between the three proposed pursuit strategies and the three proposed evasive strategies? In Ref. 8 the authors studied the evolutionary dynamics of the three pursuit strategies (P1)-(P3) playing against an environment of nonreactive deterministic or random evasive strategies such as (E2). In the following section we consider an evolutionary scenario in which the pursuit strategies coevolve with *reactive* evasive strategies (E1) and (E3) as well.

III. Evolutionary Dynamics

To gain insight into the consequences of evolutionary competition between a population of pursuers and a population of evaders, we cast the problem in the framework of evolutionary dynamics (c.f. Refs. 7,16,17). The key idea here is that individuals in a population play a certain strategy that determines their payoff or fitness. This fitness can be a function of the environment, the strategies of other individuals, the frequencies

or distribution of competing strategies in the environment (known as frequency dependence) and the density of individuals present in a region (density dependence), among other factors. Strategies with higher fitness become widespread in a population, and can eventually take over the population; strategies with lower fitness become diminished and might eventually go extinct. Here we consider frequency dependence in a competition between a population of pursuers and a population of evaders. The population of pursuers and the population of evaders are assumed to be composed of individuals playing strategies (employing control laws) (P1)-(P3) and (E1)-(E3), respectively. Fitnesses are determined by the cumulative effect of several one-on-one contests between pursuers and evaders such that a long time-to-capture for a particular contest corresponds to a high evader fitness and a low pursuer fitness.

Consider a pursuer population represented by the population vector $\boldsymbol{p} = \begin{bmatrix} p_1 & p_2 & p_3 \end{bmatrix}^T$. Here p_i, $i \in \{1,2,3\}$, corresponds to the fraction of individuals in the population playing strategy (Pi). Hence the vector $\boldsymbol{p}$ is restricted to the 2-simplex defined by $\Delta^2 = \left\{\boldsymbol{p} \mid \boldsymbol{p}^T \mathbf{1}_3 = 1 \text{ and } p_i \geq 0,\ \forall i\right\}$. Similarly, the evader population is represented by the population vector $\boldsymbol{q} = \begin{bmatrix} q_1 & q_2 & q_3 \end{bmatrix}^T$ which is also restricted to Δ^2. The fitness vectors for the pursuer and evader populations are denoted by $\boldsymbol{f_P} \in \mathbb{R}^3_+$ and $\boldsymbol{f_E} \in \mathbb{R}^3_+$ respectively, where f_{Pi} is the fitness of pursuit strategy (Pi) and f_{Ej} is the fitness of evasive strategy (Ej) . Define population mean fitness by $\widehat{f_P} = \boldsymbol{p}^T \boldsymbol{f_P}$ and $\widehat{f_E} = \boldsymbol{q}^T \boldsymbol{f_E}$.

We can now write down a discrete update equation for each population that depends on the relative fitnesses of the different strategies in that population. For transition from generation g to generation $g+1$, we have for $i = 1,2,3$ and $j = 1,2,3$:

$$\begin{aligned} p_i(g+1) &= p_i(g)\frac{f_{Pi}}{\widehat{f_P}} \\ q_j(g+1) &= q_j(g)\frac{f_{Ej}}{\widehat{f_E}}. \end{aligned} \tag{2}$$

One can verify that the equations (2) ensure that each population vector remains in the simplex Δ^2. Intuitively, strategies with fitness greater than the population mean fitness are favored. Given an expression for the fitness vectors, we can study the outcomes of the dynamics (2). As in Ref. 8 we use time-to-capture as a measure of fitness. The fitness of the set of pursuer strategies $\boldsymbol{f_P}$ depends on the distribution of evaders in the population $\boldsymbol{q}$ and $\boldsymbol{f_E}$ depends on the distribution of pursuers in the population $\boldsymbol{p}$. This implies that the equations (2) are coupled. We simulate the evolutionary dynamics (2) using Monte-Carlo calculations that determine fitnesses. We then perform a theoretical analysis.

III.A. Monte-Carlo Simulations

We follow the setup in Ref. 8 for our Monte-Carlo experiments. The important step is the construction of the capture time matrix $T \in \mathbb{R}^{3\times 3}$ such that $t_{ij} > 0$ represents the time-to-capture for pursuit strategy (Pi) competing against evasive strategy (Ej). Proposition 1 gives us that all elements of T are positive and finite. To construct T, we perform nine simulations, one for each element of T, such that each simulation has a pursuer and an evader starting from the same initial conditions. In each simulation the evader starts at the origin with a heading of zero. The pursuer's initial position is chosen from a uniform distribution on the square $[-10,10] \times [-10,10]$, and its initial heading from a uniform distribution on $\mathbb{S}^1$. The other parameters are the same for each simulation: $\eta = \mu = 10$, $\nu = .6$, $\epsilon = 0.05$, $\phi = 0.3$, $\alpha = 0.2$, and $\kappa = 2$. The results presented here remain qualitatively consistent for reasonable variations of these parameters. A detailed study of the effect of each parameter on capture times is a direction of future work.

For each generation, we compute ten time matrices T_k, $k \in \{1,\ldots,10\}$, such that each matrix corresponds to a different choice of pursuer initial conditions and evader random trajectory for column 2. The average matrix $\overline{T}$ is defined by $\overline{t_{ij}} = \dfrac{1}{10}\displaystyle\sum_{k=1}^{10} t_{kij}$. Let $\overline{T}(g)$ denote the average time matrix computed at generation g. Letting matrices $\overline{M}(g) = \overline{T}^{\,\#}(g)$ and $\overline{N}(g) = \overline{T}^{\,T}(g)$, the fitness vectors are defined by

$$\begin{aligned} \boldsymbol{f_P}(g) &= \overline{M}(g)\boldsymbol{q}(g) \\ \boldsymbol{f_E}(g) &= \overline{N}(g)\boldsymbol{p}(g). \end{aligned} \tag{3}$$

The inverse and direct relationships between the time matrix and fitness for pursuers and evaders, respectively, ensure that high capture times have asymmetric fitness consequences for pursuers and evaders. Equations (3) also encode the frequency dependence and coupling of the evolutionary dynamics (2) since the fitness of a pursuer (evader) strategy depends on the population distribution of evader (pursuer) strategies. Another way of interpreting equations (3) is from the perspective of a focal pursuer (evader) employing a specific strategy in a given generation. The expected fitness of this individual depends on expected interactions with each evasive (pursuit) strategy, which in turn depends on the population distribution of evaders (pursuers).

Equations (2) and (3) give us the necessary tools to simulate the pursuit-evasion dynamics defined on the direct product of two simplexes. This is done for a set of 50 randomly chosen pairs of initial distributions $\boldsymbol{p}(0)$ and $\boldsymbol{q}(0)$. Each set of initial conditions is propagated using equations (2) and (3) for 100 generations with new fitness matrices $\overline{M}(g)$ and $\overline{N}(g)$ calculated at each generation. The results of the simulation are plotted in Figure 3. Note that the trajectories eventually converge to the point corresponding to pure classical pursuit and pure classical evasion, i.e. $\boldsymbol{p}_{eq} = \boldsymbol{q}_{eq} = \begin{bmatrix} 1 & 0 & 0 \end{bmatrix}^T$. Further, the Monte-Carlo simulations point to an interesting and useful structure in the matrix $\overline{T}$ (and correspondingly in $\overline{M} = \overline{T}^{\#}$ and $\overline{N} = \overline{T}^{T}$) which we state below in Proposition 2 without proof.

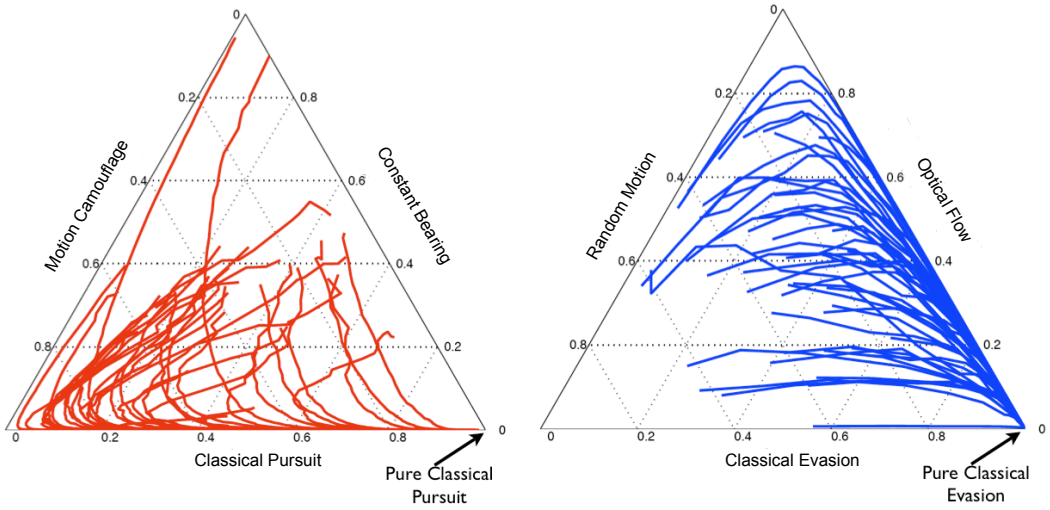

Figure 3. Monte-Carlo simulation of equations (2) and (3). The simplex on the left corresponds to pursuit strategies and the simplex on the right to evasive strategies. The corners of the simplexes mark pure strategies and points on the interior of the simplexes correspond to mixed strategies. The curves on each simplex evolve in pairs $(\boldsymbol{p}, \boldsymbol{q}) \in \Delta^2 \times \Delta^2$; there are 50 pairs in all corresponding to 50 different initial conditions $(\boldsymbol{p}(0), \boldsymbol{q}(0))$. Each pair of trajectories comprises 100 generations (iterations of equation (2)) and hence $100 \times 10 = 1000$ evaluations of matrix T. The trajectories all eventually converge to pure classical pursuit (left figure) and pure classical evasion (right figure), indicating that classical pursuit and classical evasion is the evolutionarily stable equilibrium of the dynamics.

Proposition 2. *The first column of matrix $\overline{T}$ is dominant, i.e. $\overline{t_{i1}} > \overline{t_{i2}}$ and $\overline{t_{i1}} > \overline{t_{i3}}$ for all i. Further, in the first column $\overline{t_{11}} < \overline{t_{21}}$ and $\overline{t_{11}} < \overline{t_{31}}$.*

The claim in Proposition 2 is made as a consequence of Monte-Carlo computations of matrix $\overline{T}$ and consistent observations of the proposed matrix structure. A formal proof of Proposition 2 requires careful analytical computations of capture times for the different strategies, a topic for future work. The structure of Proposition 2 provides a useful tool for analyzing the evolutionary dynamics on the direct product of two simplexes and for proving convergence properties. We investigate this in the following section.

III.B. Theoretical Analysis

For some small time step $\Delta t > 0$, we can rewrite the equations (2) as follows:

$$\frac{1}{\Delta t}\left(p_i(g+1) - p_i(g)\right) = p_i(g)\frac{f_{Pi} - \widehat{f_P}}{\Delta t\ \widehat{f_P}}$$
$$\frac{1}{\Delta t}\left(q_j(g+1) - q_j(g)\right) = q_j(g)\frac{f_{Ej} - \widehat{f_E}}{\Delta t\ \widehat{f_E}}.$$

In the limit $\Delta t \to 0$, we get

$$\dot{p_i} = p_i\frac{f_{Pi} - \widehat{f_P}}{\Delta t\ \widehat{f_P}}$$
$$\dot{q_j} = q_j\frac{f_{Ej} - \widehat{f_E}}{\Delta t\ \widehat{f_E}}.$$

Applying a further timescale change[8] we finally arrive at the set of differential equations

$$\begin{aligned}\dot{p_i} &= \frac{p_i}{\widehat{f_P}}\left(f_{Pi} - \widehat{f_P}\right)\\ \dot{q_j} &= \frac{q_j}{\widehat{f_E}}\left(f_{Ej} - \widehat{f_E}\right).\end{aligned} \tag{4}$$

Consider a constant matrix T that obeys the structure of Proposition 2. Further let $M = T^{\#}$ and $N = T^T$. Defining fitness vectors $\boldsymbol{f_P} = M\boldsymbol{q}$ and $\boldsymbol{f_E} = N\boldsymbol{p}$ analogous to equation (3), and substituting into (4) we get

$$\begin{aligned}\dot{p_i} &= \frac{p_i}{\boldsymbol{p}^T M\boldsymbol{q}}\left((M\boldsymbol{q})_i - \boldsymbol{p}^T M\boldsymbol{q}\right)\\ \dot{q_j} &= \frac{q_j}{\boldsymbol{q}^T N\boldsymbol{p}}\left((N\boldsymbol{p})_j - \boldsymbol{q}^T N\boldsymbol{p}\right).\end{aligned} \tag{5}$$

Equations (5) are a form of the replicator dynamics[18] for two interacting populations with fitnesses defined by linear functions of the population distributions. Critical to arriving at equations (5) is the assumption that T is constant and thus M and N are constant. This is motivated by a 'law of large numbers' argument.[8] Further, the assumption makes the analysis of equations (5) tractable, and hence allows us to formally investigate the convergence shown in the Monte-Carlo experiments.

The system of equations (5) is a four-dimensional system evolving on $\Delta^2 \times \Delta^2$. There are several possible solutions of the dynamics on these simplexes. For instance, all vertex pairs (pairs of pure strategies) are fixed points. Further, a strategy that is initially absent does not ever emerge, i.e., $p_i(0) = 0 \implies p_i(t) = 0,\ \forall t$, and the same holds for q_j (replicator dynamics are said to be *non-innovative* – we do not consider mutations here). Given the structure of the matrices M and N from Proposition 2, we investigate the dynamics of equations (5).

In order to investigate the coupled replicator dynamical system (5), we first study the simpler single population replicator dynamics given by

$$\dot{q_i} = \frac{q_i}{\boldsymbol{q}^T\boldsymbol{f}}\left(f_i - \boldsymbol{q}^T\boldsymbol{f}\right), \text{ for } i = 1, 2, 3. \tag{6}$$

The fitness functions for the system of equations (6) are assumed to satisfy the following properties:

- *Property 1:* $f_i \equiv f_i(t)$, $i = 1, 2, 3$, are each distinct functions of time, i.e., $f_i \neq f_j$ pointwise. If this were not the case then populations i and j would be indistinguishable from the perspective of evolutionary dynamics.
- *Property 2:* The functions $f_i(t)$ are each globally Lipschitz, bounded and positive for all $t \geq 0$.
- *Property 3:* The functions $f_i(t)$ have a single dominant fitness; without loss of generality, $f_3(t) > f_2(t)$ and $f_3(t) > f_1(t)$ for all $t \geq 0$.

Lemma 1. *Assume initial conditions are restricted to the domain* $D = \{\boldsymbol{q} \in \Delta^2 | q_3 > 0\}$. *The dynamics* (6)*, satisfying Properties 1-3, have a unique asymptotically stable equilibrium point* $\boldsymbol{q}_{eq} = \begin{bmatrix} 0 & 0 & 1 \end{bmatrix}^T$ *attracting all initial conditions in* D.

Proof. We first show that the domain D is an invariant set with respect to the dynamics (6). All boundaries of D are clearly invariant since $q_i \in \{0,1\} \implies \dot{q}_i = 0$. Thus Δ^2 is invariant. We have left to show that $q_3(0) > 0 \implies q_3(t) > 0$ for all $t > 0$. To do this consider

$$\dot{q}_3 = \frac{q_3 f_3}{\boldsymbol{q}^T \boldsymbol{f}} - q_3 \geq -q_3.$$

This implies for all $t > 0$,

$$q_3(t) \geq q_3(0) e^{-t} > 0.$$

Using the constraint $\boldsymbol{q}^T \mathbf{1}_3 = 1$, we restate the dynamics (6) as a two-dimensional system,

$$\begin{aligned} \dot{q}_1 &= \frac{q_1}{\widehat{f}} \left(f_{31}(t)(q_1 - 1) + f_{32}(t) q_2 \right) \\ \dot{q}_2 &= \frac{q_2}{\widehat{f}} \left(f_{32}(t)(q_2 - 1) + f_{31}(t) q_1 \right), \end{aligned} \tag{7}$$

where $f_{32}(t) = f_3(t) - f_2(t) > 0$, $f_{31}(t) = f_3(t) - f_1(t) > 0$, and $\widehat{f} = \boldsymbol{q}^T \boldsymbol{f} = f_3 - q_1 f_{31} - q_2 f_{32}$. Also $(q_1, q_2) \in D$ where the invariant domain D is rewritten as $D = \{(q_1, q_2) \mid q_1 \geq 0, q_2 \geq 0, q_1 + q_2 < 1\}$. One can check that the only three equilibrium points of the system (7) in Δ^2 (given properties (1)-(3)) are the vertices $(q_{eq1}, q_{eq2}) = (0,0), (0,1), (1,0)$, of which $(0,0)$ is the only equilibrium in D.

Linearization about the $(0,0)$ equilibrium gives the dynamics,

$$\begin{bmatrix} \dot{q}_1 \\ \dot{q}_2 \end{bmatrix} = \begin{bmatrix} -f_{31}/f_3 & 0 \\ 0 & -f_{32}/f_3 \end{bmatrix} \begin{bmatrix} q_1 \\ q_2 \end{bmatrix}.$$

This non-autonomous linear system in diagonal form can be solved easily as

$$q_i(t) = q_i(0) \exp\left(- \int_0^t \frac{f_{3i}(t)}{f_3(t)} dt \right), \; i = 1, 2.$$

For $i = 1, 2$, $\lim_{t \to \infty} q_i(t) = 0$ and hence the $(0,0)$ equilibrium point of the non-autonomous system (7) is locally asymptotically stable by Theorem 4.13 of Ref. 19.

To prove that the invariant domain D is the region of attraction for the asymptotically stable $(0,0)$ equilibrium point of (7), we use a Lyapunov function $V = q_1 + q_2$. V is positive definite on D with a unique minimum: $V = 0 \iff q_1 = q_2 = 0$. We compute

$$\dot{V} = \dot{q}_1 + \dot{q}_2 = \frac{1}{\widehat{f}} (q_1 f_{31} + q_2 f_{32})(q_1 + q_2 - 1) < 0.$$

Since $\dot{V}$ is negative definite on the domain D, by Theorem 4.9 of Ref. 19 we have that D is the region of attraction for the equilibrium point $q_{eq1} = 0, q_{eq2} = 0$ (and $q_{eq3} = 1$). Hence the equilibrium point $\boldsymbol{q}_{eq} = \begin{bmatrix} 0 & 0 & 1 \end{bmatrix}^T$ is the asymptotically stable limit for all $\boldsymbol{q}(0) \in D$. □

Note that the case of Lemma 1 with each f_i constant is considered in Ref. 8. We now return to the coupled two populations set of equations (5) and state the main theorem of this section. Here we employ the dominant structure of matrix T from Proposition 2 to prove convergence.

Theorem 1. *Assume initial conditions are restricted to the domain* $D_2 = \{(\boldsymbol{p}, \boldsymbol{q}) \in \Delta^2 \times \Delta^2 | p_1 > 0, q_1 > 0\}$. *Let matrix* T *satisfy Proposition 2 with* $M = T^{\#}$ *and* $N = T^T$. *Then, the coupled replicator dynamics* (5) *have a unique asymptotically stable equilibrium point* $\boldsymbol{p}_{eq} = \boldsymbol{q}_{eq} = \begin{bmatrix} 1 & 0 & 0 \end{bmatrix}^T$ *attracting all initial conditions in* D_2.

Proof. The invariance of the domain D_2 with respect to the dynamics (5) follows from the invariance of the domain D in the proof of Lemma 1. The column dominant structure of matrix T implies that the first element of the fitness vector $\boldsymbol{f}_E = N\boldsymbol{p} = T^T\boldsymbol{p}$ is dominant. That is, regardless of the population distribution $\boldsymbol{p}$ at any time instant, $f_{E1} > f_{E2}$ and $f_{E1} > f_{E3}$. Hence we can apply Lemma 1 to conclude that regardless of the evolution of the population vector $\boldsymbol{p}$, the population vector $\boldsymbol{q}$ will asymptotically converge to $\boldsymbol{q}_{eq} = \begin{bmatrix} 1 & 0 & 0 \end{bmatrix}^T$.

Asymptotic stability implies that for every $\epsilon > 0$ there exists a time $t_1 \geq 0$ such that $t > t_1 \implies \|\boldsymbol{q} - \boldsymbol{q}_{eq}\| < \epsilon$. Based on the calculations in Lemma 2 of the Appendix, we let

$$\epsilon = \min\left\{ \frac{2(m_{11} - m_{21})}{(m_{11} - m_{21}) + \|M\|_1}, \frac{2(m_{11} - m_{31})}{(m_{11} - m_{31}) + \|M\|_1} \right\}.$$

For this choice of ϵ we are guaranteed that for all $t > t_1$ the fitness vector $\boldsymbol{f_P} = M\boldsymbol{q}$ preserves the ordering $f_{P1} > f_{P2}$ and $f_{P1} > f_{P3}$. Hence we can apply Lemma 1 again to the dynamics of $\boldsymbol{p}$ to conclude that after time t_1, the population vector $\boldsymbol{p}$ will also asymptotically converge to $\boldsymbol{p}_{eq} = \begin{bmatrix} 1 & 0 & 0 \end{bmatrix}^T$. □

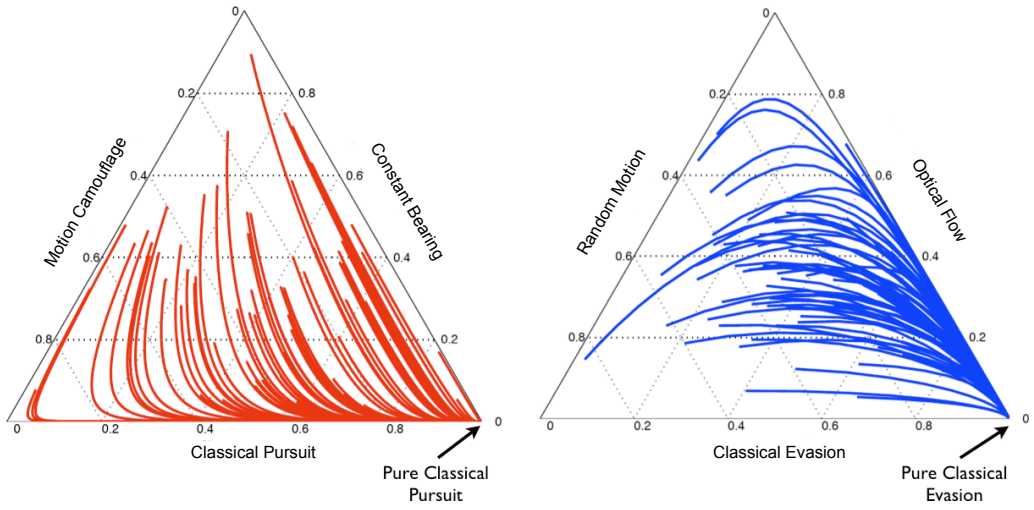

Figure 4. Simulation of smooth dynamics (5). The capture time matrix T is chosen to be the mean of 50 Monte-Carlo computations of capture time matrices T_k; $M = T^{\#}$ and $N = T^T$. The plot on the left shows the population vector $\boldsymbol{p}$ and the one on the right shows $\boldsymbol{q}$. 50 pairs of trajectories are plotted with initial conditions chosen from a uniform random distribution on the space of two simplexes $\Delta^2 \times \Delta^2$. Comparisons to the Monte-Carlo simulations in Figure 3 show strong similarities, illustrating the value of our analytical approach.

In Figure 4 we simulate the dynamics in equations (5), for a particular calculation of matrix T, showing smooth convergence to the unique stable equilibrium. This can be compared to the Monte-Carlo simulations of Figure 3. From a game-theoretic perspective, the stable equilibrium point corresponds to the single unique pure Nash equilibrium of the bi-matrix game, for payoff matrices M and N.

In this section we have performed a computational and theoretical analysis of the evolutionary dynamics corresponding to the competition between a population of pursuers and a population of evaders, each having three strategies. We have shown convergence to a unique stable pure-strategy equilibrium corresponding to classical pursuit and classical evasion. This differs from the solution in Ref. 8, where the authors study the three pursuit strategies as a 'game against nature', each competing independently against nonreactive evasive strategies. There the evolutionary dynamics converge to the motion camouflage pursuit strategy. In the present paper, we look at competition of pursuers with a reactive set of evaders, which introduces a rich set of possibilities for evolutionary outcomes. Indeed, by comparison to the results of Ref. 8, we see that making available alternative evader strategies affects the evolved strategies for both pursuers and evaders. We note that one need not restrict to the three chosen pursuit or evasive strategies; other choices of strategies may be appropriate depending on the context. Regardless of the set of strategy choices, evolutionary dynamics provides a powerful tool to determine the outcome of such pursuit-evasive interactions in natural and engineered settings.

We now shift focus to employing pursuit and evasive behaviors for collective motion. In the following section we examine classical pursuit and classical evasion as this pair constitutes the evolutionary equilibrium of our strategy space.

IV. Collective Motion

The multi-agent dynamics described in this section are motivated in part by work done by Bazazi et al[11] (further analyzed by Romanczuk et al[20]). These authors study social forging in groups of cannibalistic migratory locusts: individuals pursue other conspecifics in front of them and evade individuals approaching from behind. We do not intend to mimic the collective dynamics observed in Ref. 11, rather we study the outcomes of collective dynamics of steered particles exhibiting classical pursuit and evasive behaviors simultaneously.

Consider a system of N agents indexed by $j = 1, \ldots, N$, each having position $r_j = x_j + iy_j$ and heading θ_j. The agents are steered particles with constant speed $v > 0$ and steering control u_j. Similar to equations (1), the kinematics of the agents are given by

$$\dot{r}_j = ve^{i\theta_j}, \qquad \dot{\theta}_j = u_j. \tag{8}$$

For each agent we define baseline vectors $b_{j+} = r_{j+1} - r_j$ and $b_{j-} = r_{j-1} - r_j$. Note that $j+1$ and $j-1$ are defined mod N; i.e., $b_{N+} = r_1 - r_N$ and $b_{1-} = r_N - r_1$. The control law u_j is given by

$$\begin{aligned} u_j &= u_{jP} + u_{jE} \\ &= K \left\langle ie^{i\theta_j}, \frac{b_{j+}}{\|b_{j+}\|} \right\rangle - \beta K \left\langle ie^{i\theta_j}, \frac{b_{j-}}{\|b_{j-}\|} \right\rangle, \end{aligned} \tag{9}$$

for scalar gain $K > 0$ and scaling parameter $\beta > 0$. The first term in the control law (9) is a classical pursuit term, with agent j pursuing agent $j+1$ by attempting to align its heading with the baseline between j and $j+1$ (i.e., b_{j+}). The second term is an evasive term with agent j evading agent $j-1$ by attempting to align its heading anti-parallel to the baseline between j and $j-1$. The dynamics correspond to a cyclical interaction (sensing) topology between agents as illustrated in Figure 5.

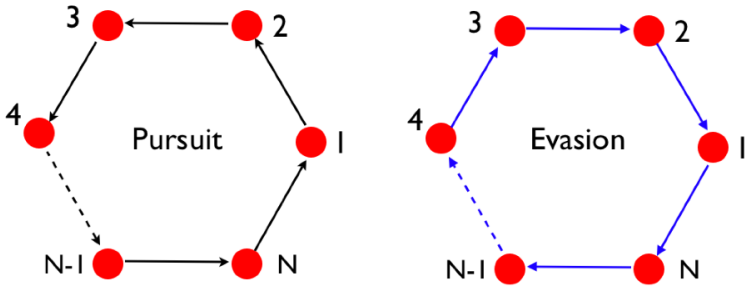

Figure 5. Sensing topology for cyclic pursuit and evasion. An arrow from agent j to k should be read as 'j senses k'. Agents pursue the agent immediately ahead and evade the agent immediately behind.

Simulations of the collective dynamics show several interesting outcomes:

- For $\beta < 1$, stable circular motions exist with agents traveling equally spaced around a circle of radius $\frac{v}{K(1-\beta)\sin(\pi/N)}$. This is illustrated for a formation of $N = 8$ agents in Figure 6.
- For $\beta \geq 1$ we observe a bifurcation. Specifically, the steady circular motions disappear and the agents diverge into an incoherent state as shown in Figure 7.
- For $\beta < 1$, the circular motions are not the only stable steady motions. We also observe convergence to regular figure eight weaving patterns as illustrated in Figure 8; the initial conditions in Figure 8 are the only change from the simulation in Figure 6. Observation of weaving patterns was also reported for pure cyclic pursuit.[12]

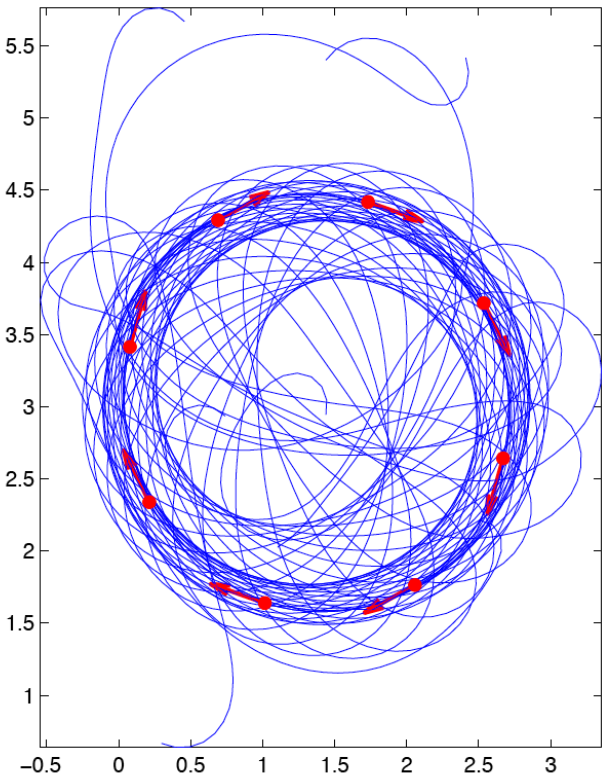

Figure 6. Convergence to a circle for a group of $N = 8$ agents with $\beta < 1$. Parameters are $K = 5$, $v = 1$ and $\beta = 0.5$.

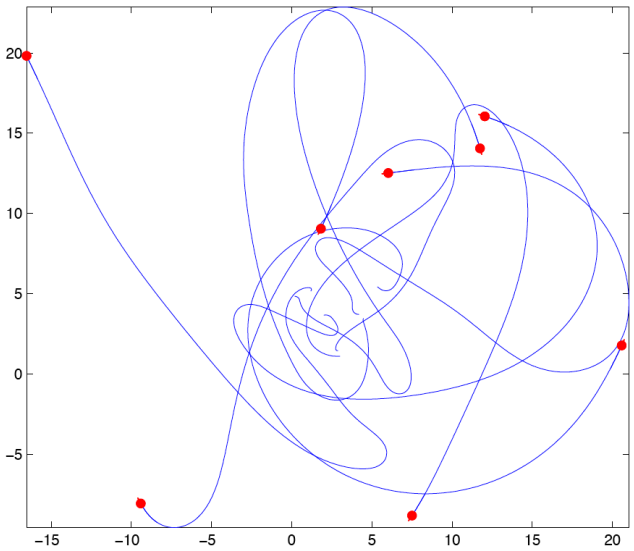

Figure 7. Divergence into an incoherent state for pursuit-evasion dynamics with $\beta \geq 1$, i.e., evasion is stronger than pursuit. Parameters are $K = 5$, $v = 1$ and $\beta = 1.2$.

These results suggest that for stable circular motions to emerge from cyclic pursuit and evasion, the pursuit action must be stronger than the evasive action. This is consistent with Ref. 20 in which stable vortices for pursuit agents are observed. The authors[20] note that 'pursuit facilitates the formation of clusters' (cohesion) whereas 'escape (evasion) leads to a homogenization of density' (dispersion).

In the case of a large number of agents following the pursuit-evasion dynamics (8),(9), the agents settle

quickly into a cyclical chain-like formation. The chain starts off with an arbitrary shape (dependent on initial conditions) and continually deforms (changes shape) on a slow time scale as illustrated in Figure 9. Simulations run for extended time do not show convergence of the formation to a regular motion; instead they show the continued slow deformation of the chain. An analysis of the chain-like formations as shown in Figure 9, perhaps using continuum methods, is a topic of future work.

In this section, we have used simulation to explore the classical pursuit and evasion control laws. An extension to other pursuit and evasion strategies proposed in this paper ((P2),(P3),(E3)) may lead to a richer set of steady motions. It is also of interest to consider a heterogeneous system with distinct subsets of agents employing distinct pursuit and evasive behaviors in a cyclical (or other) interconnection topology.

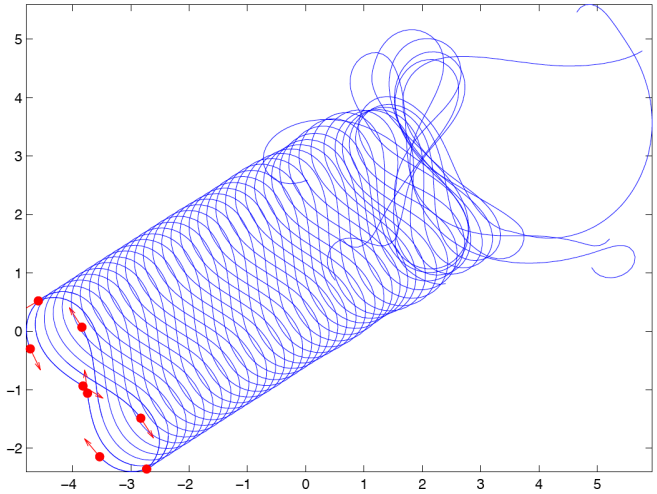

Figure 8. Weaving figure eight solution for $N = 8$ agents and $\beta < 1$. Parameters are $K = 5$, $v = 1$ and $\beta = 0.5$.

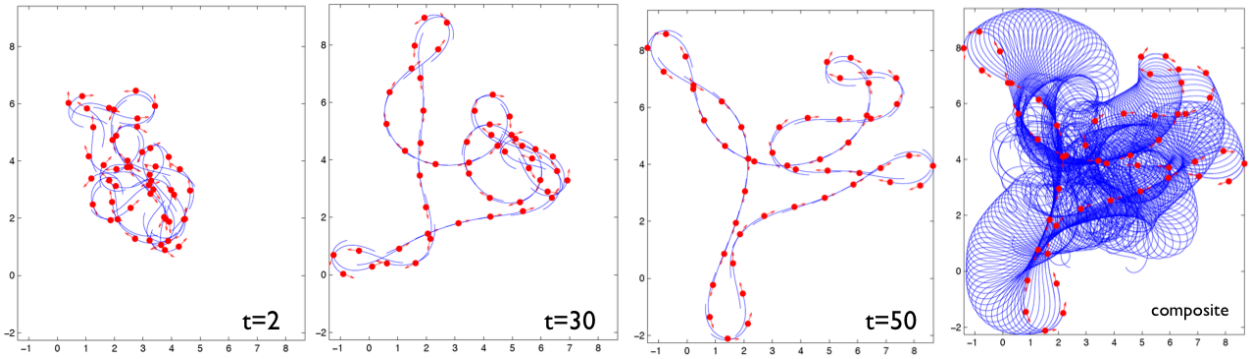

Figure 9. Chains for large N, here $N = 50$. The plots from left to right show snapshots at indicated times. The plot on the right is a composite showing trajectories of all agents over time. Parameters are $K = 5$, $v = 1$ and $\beta = 0.5$.

V. Conclusion

In this paper we have considered an evolutionary game of three strategies of pursuit against three strategies of evasion, two of which are reactive. Monte-Carlo simulations of the evolutionary dynamics, involving fitness computations for the interactions between the different pursuer and evader pairs, show convergence to a stable equilibrium of classical pursuit and classical evasion. Using the structure of the fitness matrices as observed in these simulations, we analytically prove the convergence of replicator dynamics to the same classical pursuit and classical evasion equilibrium as in our Monte-Carlo simulations. This effort builds on prior work[8] where it was shown for the same three pursuit strategies but with nonreactive evasion strategies, that replicator dynamics converge to motion camouflage pursuit. Our result provides an interesting contrast to

the earlier result[8] and further illustrates that the consequences of evolutionary dynamics depend significantly on the space of strategies considered. Evolutionary dynamics are a useful tool for finding Nash equilibria and evolutionary stable strategies in complex interactions and games. Using strategy spaces different again from those in this paper may lead to a richer set of outcomes, including, for example, mixed strategy solutions as opposed to the pure strategy equilibrium shown here.

Motivated by the outcome of the evolutionary game studied in this paper and by the behavior of cannabilistic locusts, we have investigated a novel control scheme involving agents performing simultaneous pursuit and evasion on cyclical interaction topologies. In the case that the pursuit gain is larger than the evasion gain, simulations indicate local convergence to circular motion formations of specified radius as well as local convergence to more complex weaving patterns. Exploring the use of different pursuit and evasive behaviors and corresponding collective outcomes is a topic of future work.

Appendix

Lemma 2. *Let* $\boldsymbol{q} \in \Delta^2$, $\boldsymbol{q_{eq}} = \begin{bmatrix} 1 & 0 & 0 \end{bmatrix}^T$ *and* $\boldsymbol{f_P} = M\boldsymbol{q}$, *where* $M = T^{\#}$ *and* T *satisfies Proposition 2. Then* $\|\boldsymbol{q} - \boldsymbol{q_{eq}}\| < \epsilon \implies f_{P1} > f_{P2}$ *and* $f_{P1} > f_{P3}$, *where* $\epsilon \leq min\left\{ \frac{2(m_{11}-m_{21})}{(m_{11}-m_{21})+\|M\|_1}, \frac{2(m_{11}-m_{31})}{(m_{11}-m_{31})+\|M\|_1} \right\}$.

Proof. $\|\boldsymbol{q} - \boldsymbol{q_{eq}}\|_1 < \epsilon \implies q_1 > 1 - \frac{\epsilon}{2}$, $q_2 < \frac{\epsilon}{2}$ and $q_3 < \frac{\epsilon}{2}$. Suppose that

$$
\begin{aligned}
& \epsilon \leq \frac{2(m_{11} - m_{21})}{(m_{11} - m_{21}) + \|M\|_1} \\
\implies & \epsilon < \frac{2(m_{11} - m_{21})}{(m_{11} - m_{21}) + (m_{22} + m_{23})} \\
\implies & (m_{11} - m_{21}) \left(1 - \frac{\epsilon}{2}\right) > (m_{22} + m_{23}) \frac{\epsilon}{2} \\
\implies & (m_{11} - m_{21}) q_1 > m_{22} q_2 + m_{23} q_3 \\
\implies & (m_{11} - m_{21}) q_1 > m_{22} q_2 + m_{23} q_3 - m_{12} q_2 - m_{13} q_3 \\
\implies & \begin{bmatrix} m_{11} & m_{12} & m_{13} \end{bmatrix}^T \boldsymbol{q} > \begin{bmatrix} m_{21} & m_{22} & m_{23} \end{bmatrix}^T \boldsymbol{q}, \text{ or } f_{P1} > f_{P2}.
\end{aligned} \tag{10}
$$

Similarly one can show that

$$
\epsilon \leq \frac{2(m_{11} - m_{31})}{(m_{11} - m_{31}) + \|M\|_1} \implies f_{P1} > f_{P3}. \tag{11}
$$

Combining (10) and (11) we get the desired result.

□

Acknowledgments

The authors gratefully acknowledge support from ONR grant N00014-09-1-1074. DP is also supported by the Gordon Wu and Martin Summerfield Princeton graduate engineering fellowships.

References

[1]Isaacs, R., *Differential Games: A Mathematical Theory with Applications to Warfare and Pursuit, Control and Optimization*, Dover Publications, 1999.

[2]Pontani, M. and Conway, B., "Optimal interception of evasive missile warheads: numerical solution of the differential game," *Journal of Guidance Control and Dynamics*, Vol. 31, No. 4, 2008, pp. 1111–1122.

[3]Karelahti, J., Virtanen, K., and Raivio, T., "Near-optimal missile avoidance trajectories via receding horizon control," *Journal of Guidance Control and Dynamics*, Vol. 30, No. 5, 2007, pp. 1287.

[4]Raivio, T. and Ehtamo, H., "Visual aircraft identification as a pursuit-evasion game," *Journal of Guidance, Control and Dynamics*, Vol. 23, No. 4, 2000, pp. 701–708.

[5]Neuman, F., "On the approximate solution of complex combat games." *Journal of Guidance, Control, and Dynamics*, Vol. 13, No. 1, 1990, pp. 128–136.

[6]Nahin, P., *Chases and Escapes: The Mathematics of Pursuit and Evasion*, Princeton University Press, 2007.

[7]Smith, J., *Evolution and the Theory of Games*, Cambridge University Press, 1982.

[8]Wei, E., Justh, E., and Krishnaprasad, P., "Pursuit and an evolutionary game," *Proceedings of the Royal Society A*, Vol. 465, No. 2105, 2009, pp. 1539.

[9]Justh, E. and Krishnaprasad, P., "Steering laws for motion camouflage," *Proceedings of the Royal Society A*, Vol. 462, No. 2076, 2006, pp. 3629.

[10]Ghose, K., Horiuchi, T. K., Krishnaprasad, P. S., and Moss, C. F., "Echolocating bats use a nearly time-optimal strategy to intercept prey," *PLoS Biology*, Vol. 4, No. 5, 04 2006, pp. e108.

[11]Bazazi, S., Buhl, J., Hale, J., Anstey, M., Sword, G., Simpson, S., and Couzin, I., "Collective motion and cannibalism in locust migratory bands," *Current Biology*, Vol. 18, No. 10, 2008, pp. 735–739.

[12]Marshall, J., *Coordinated autonomy: Pursuit formations of multivehicle systems*, Ph.D. thesis, University of Toronto Toronto, Ontario, Canada, 2005.

[13]Marshall, J., Broucke, M., and Francis, B., "Pursuit formations of unicycles," *Automatica*, Vol. 42, No. 1, 2006, pp. 3–12.

[14]Marshall, J., Broucke, M., and Francis, B., "Formations of vehicles in cyclic pursuit," *IEEE Transactions on Automatic Control*, Vol. 49, No. 11, 2004, pp. 1963–1974.

[15]Srinivasan, M. V. and Zhang, S., "Visual motor computations insects," *Annual Review of Neuroscience*, Vol. 27, No. 1, 2004, pp. 679–696.

[16]Nowak, M., *Evolutionary Dynamics: Exploring the Equations of Life*, The Belknap Press of Harvard University Press, 2006.

[17]Hofbauer, J. and Sigmund, K., "Evolutionary game dynamics," *Bulletin-American Mathematical Society*, Vol. 40, No. 4, 2003, pp. 479–520.

[18]Taylor, P. and Jonker, L., "Evolutionary stable strategies and game dynamics," *Mathematical Biosciences*, Vol. 40, No. 1-2, 1978, pp. 145–156.

[19]Khalil, H., *Nonlinear Systems*, Prenctice Hall, 2002.

[20]Romanczuk, P., Couzin, I., and Schimansky-Geier, L., "Collective motion due to individual escape and pursuit response," *Physical Review Letters*, Vol. 102, No. 1, 2009, pp. 10602.